

Dielectric Behavior Induced by Vitamin E and Electron Beam Irradiation in Ultra High Molecular Weight Polyethylene

Jose Antonio Puértolas,¹ Maria Jose Martínez-Morlanes,¹ Roberto Teruel,² Alfonso Martinez-Felipe,² Ebru Oral,³ Francisco Javier Pascual,^{1,4} Amparo Ribes²

¹Department of Materials Science and Technology, Universidad de Zaragoza, Zaragoza, Spain

²Institute of Materials Technology, Universitat Politècnica de Valencia, Valencia, Spain

³Harris Orthopaedic Laboratory, Massachusetts General Hospital, Boston, Massachusetts

⁴Centro Universitario de la Defensa de Zaragoza, Academia General Militar, Zaragoza, Spain

Correspondence to: J. A. Puértolas (E-mail: japr@unizar.es)

ABSTRACT: Radiation cross-linked ultra high molecular weight polyethylenes (UHMWPEs) have been successfully used as wear resistant bearing surfaces in total joint arthroplasty. A recent development in this field is the incorporation of the antioxidant vitamin E into radiation cross-linked UHMWPE. This study investigates the effects of radiation cross-linking and vitamin E incorporation on the dielectric behavior of UHMWPE. The dielectric relaxations of virgin and 0.1 wt % vitamin E-blended UHMWPE and their irradiated counterparts (up to 300 kGy dose) were investigated. To determine the effect of vitamin E content alone, vitamin E-loaded UHMWPEs were used. The results showed that radiation cross-linking and vitamin E content both increased dielectric polarization in UHMWPE and under some conditions induced electrical conductivity. This result is significant because it shows that the conductive response of UHMWPE-bearing surfaces may depend on manufacturing processes and additives. © 2014 Wiley Periodicals, Inc. *J. Appl. Polym. Sci.* **2014**, *131*, 40844.

KEYWORDS: biomaterials; crosslinking; dielectric properties

Received 12 January 2014; accepted 7 April 2014

DOI: 10.1002/app.40844

INTRODUCTION

Dielectric relaxation spectroscopy is a powerful tool to study the molecular dynamics in polymers.¹ This technique has also been applied to polyethylenes to understand the relaxation processes and to obtain the dielectric performance in applications where the dielectric insulation is a relevant parameter. In spite of the nonpolar character of this molecular structure, several complex relaxations named conventionally α , β , and γ have been reported in the literature from higher to lower temperature due to the presence of other traces or polar groups in the polymer chain.^{2–4} These units are introduced during the synthesis of the powder or during the consolidation process at high temperature and pressure. High density, low density, or linear low density polyethylenes have been extensively studied in order to know the influence that different processes like crystallization, aging, irradiation, or the presence of antioxidants, blends, reinforcements or nanoreinforcements produce to the aforementioned relaxations.^{5–8} In contrast to these studies related to polyethylenes, few works appeared in the literature concerning the dielectric behavior of ultra high molecular weight polyethylene (UHMWPE), which presents a low dielectric constant and dielectric loss tangent.

UHMWPE is a polymer that presents characteristics such as an excellent mechanical and tribological performance, high wear resistance, chemical inertness, and biocompatibility, which have been exploited in different industrial areas and also as bearing parts in total joint replacements.⁹ Besides, UHMWPE is a polyolefin with an effective behavior in radiation shielding and therefore with potential application for spacecraft industry or radiation-protective materials for personal and electronic equipments.¹⁰

Reinforced composite UHMWPE matrices have been developed for application in fields related to cosmic, proton, X-rays, electron, or gamma irradiation devices.^{11–13} On the other hand, electron beam irradiation process has been applied to UHMWPEs used as joint replacement parts to obtain a good sterilization method and to enhance the wear resistance behavior by crosslinking the polymer chains.^{14,15} The introduction of antioxidants, like α -tocopherol (vitamin E), in UHMWPE by blending or diffusion, has been used as chemical stabilization because vitamin E exhibits a scavenger effect to the free radical induced by the irradiation. Electron beam irradiation and vitamin E incorporation are being used to obtain first and second generation of commercially highly cross-linked polyethylenes.^{16,17}

Table I. Influence of Gamma Irradiation Doses and Vitamin E Content on Thermal Parameters of Electron Beam-Irradiated GUR1050VE0.1 and Vitamin E-Diffused GUR1050

| | Crystallinity (%) | Transition temperature (°C) |
|------------------|-------------------|-----------------------------|
| Doses (kGy) | | |
| 0 | 52.5 ± 1.0 | 134.3 ± 0.2 |
| 75 | 56.5 ± 0.5 | 137.0 ± 0.1 |
| 150 | 56.8 ± 1.8 | 138.3 ± 0.1 |
| 225 | 57.7 ± 0.9 | 139.5 ± 0.1 |
| 300 | 56.2 ± 3.1 | 140.0 ± 0.5 |
| Vitamin E (wt %) | | |
| 0 | 50.3 ± 0.9 | 134.3 ± 0.2 |
| 1.5 | 49.8 ± 1.0 | 134.2 ± 0.5 |
| 4.4 | 46.8 ± 0.7 | 138.3 ± 0.3 |
| 7.9 | 45.3 ± 0.7 | 137.9 ± 0.1 |

This study analyzes the changes in the dielectric properties and in the molecular dynamic of the UHMWPE with the incorporation of different vitamin E concentrations and under different electron beam irradiation dose.

EXPERIMENTAL

The raw material used in this study was medical-grade GUR1050 UHMWPE (Orthoplastics, UK). Vitamin E was incorporated in this polymer by blending and diffusion. The first method consisted of mixing UHMWPE powder with vitamin E at 0.1 wt %. Prior to mixing, vitamin E was dissolved in isopropyl alcohol, and the solution was mixed and stirred with the UHMWPE powder to make a homogeneous blend with a concentration of 2 wt % (weight percent). This blend was dried in a convection oven under vacuum at 60°C for 7 days and diluted with GUR1050 powders into 0.1 wt %. Finally, the last step consisted of consolidating the mixture into 9.5-mm-thick pucks under a specific program of temperature and pressure. To study the irradiation effects, these molded blocks were subsequently irradiated by electron beam to 75, 150, 225, and 300 kGy (MT Cambridge, MA). After irradiation, all the specimens were maintained at -20°C in a subzero freezer until they were measured. Thus, hereafter, these materials will be referred to as GUR1050VE0.1-X kGy, where X is the former irradiation doses.

On the other hand, with the aim to study the effects of higher vitamin E concentrations, 0.2 mm sections were microtomed from the compression-molded GUR1050 and soaked in a bath of vitamin E (α -tocopherol, Aldrich Chemicals) at 120°C in a nitrogen gas atmosphere for different times. At the end of the doping process, samples were taken out of the vitamin E bath, cleaned, and subsequently homogenized at 120°C for 24 h in nitrogen. In this case, the samples chosen for this study corresponded to concentrations of α -tocopherol of 1.4, 4.4, and 7.9 wt %. These materials will be designated as GUR1050-VEY%, where Y is the former vitamin E concentrations.

Differential scanning calorimetry was performed according to the ASTM F2625-10 standard¹⁸ to assess thermal properties,

namely crystallinity and melting and transition temperatures. Thus, three specimens ($n = 3$) per material group were heated from 20°C to 200°C at a rate of 10°C/min in a differential scanning calorimeter (Perkin Elmer). Melting temperature, transition temperature, and crystallinity were obtained for each material.

Dielectric measurements were performed using a dielectric spectrometry setup (Novocontrol BDS4000), which includes a two-terminal dielectric cell, a frequency response analyzer (Solartron 1250), and a high-impedance preamplifier of variable gain. The complex dielectric constant was obtained by sweeping the frequency range 0.01 Hz to 1 MHz at different stabilized temperatures by heating from -70°C to 120°C in temperature steps of 6°C. The samples were disks of a 0.2-mm thickness, which were held between the condenser plates (golden brass circular electrodes with a diameter of 11 mm).

The analysis was conducted through the complex dielectric permittivity $\epsilon^* = \epsilon' - i\epsilon''$, taking into account the real (ϵ') and imaginary (ϵ'') parts, as well as $\tan \delta = \epsilon''/\epsilon'$. The results were

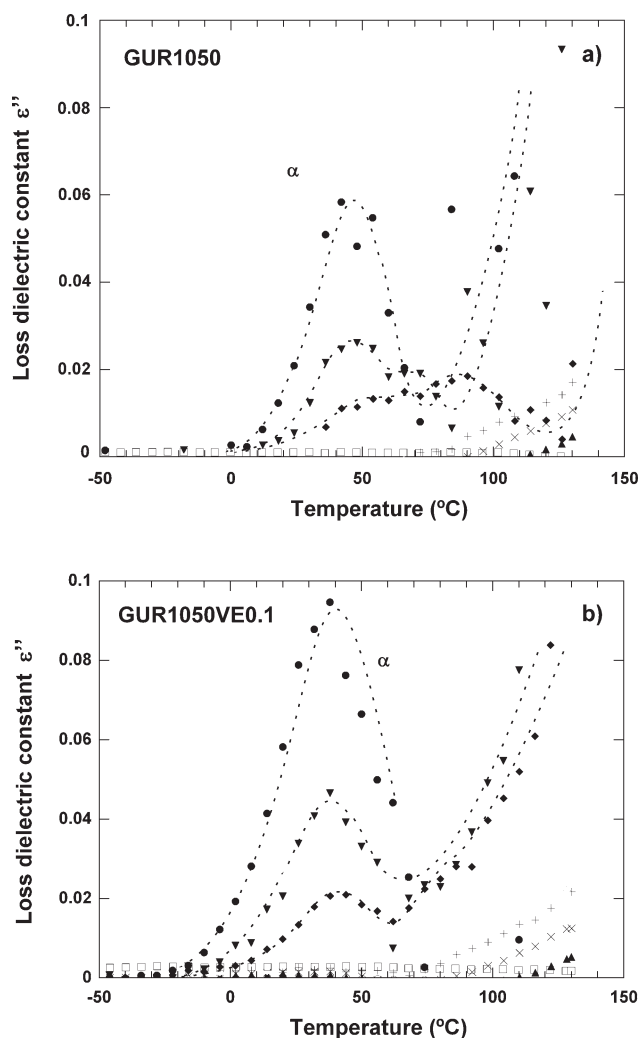


Figure 1. Temperature dependence of the imaginary part, $\epsilon''(T)$, in (a) GUR1050 and (b) GUR1050VE0.1 at different frequencies: (\square) 3×10^4 , (\circ) 3×10^3 , (\blacktriangle) 30, (\times) 10, ($+$) 3, (\blacklozenge) 0.3, (\blacktriangledown) 0.1, and (\bullet) 0.03 Hz.

Table II. Influence of Electron Beam Irradiation on AC Conductivity Parameters Obtained by eq. (4) in GUR1050VE0.1-X kGy

| T (°C) | log(σ_0) (S cm ⁻¹) | | | | S | | | |
|--------|---|---------|---------|---------|-------|---------|---------|---------|
| | 0 kGy | 150 kGy | 225 kGy | 300 kGy | 0 kGy | 150 kGy | 225 kGy | 300 kGy |
| 130 | -13.72 | | -12.09 | -11.80 | 1.00 | | 0.75 | 0.85 |
| 123 | -13.95 | | -12.11 | -12.10 | 0.93 | | 0.74 | 0.87 |
| 117 | -14.05 | | -12.49 | -12.34 | 0.97 | | 0.86 | 0.86 |
| 111 | -14.07 | | -12.88 | -12.56 | 1.00 | | 0.89 | 0.86 |
| 105 | -15.12 | -13.21 | -12.95 | -13.35 | 1.00 | 0.91 | 0.86 | 0.76 |
| 99 | | -13.36 | -13.35 | -12.96 | | 1.00 | 0.76 | 0.89 |
| 93 | | -13.49 | -13.29 | -13.14 | | 1.00 | 0.84 | 0.85 |
| 87 | | -13.67 | -13.07 | -13.30 | | 0.90 | 0.89 | 0.84 |
| 81 | | -13.78 | -13.32 | -13.50 | | 1.00 | 0.91 | 0.78 |
| 75 | | -14.02 | -13.61 | -13.67 | | 1.00 | 0.87 | 1.00 |
| 69 | | -14.40 | -13.95 | -14.07 | | 0.93 | 0.85 | 0.68 |
| 63 | | -14.66 | -14.18 | -14.27 | | 1.00 | 1.00 | 0.76 |
| 57 | | -14.96 | -14.55 | -14.46 | | 1.00 | 0.97 | 0.78 |
| 51 | | -14.97 | -15.76 | -14.55 | | 1.00 | 1.00 | 0.87 |

expressed in the frequency (f) and the temperature (T) domains. The dielectric relaxations were analyzed in the isotherms by fitting the response in the frequency domain to Havriliak–Negami (HN) curves [eq. (1)]^{19–21}:

$$\varepsilon^* - \varepsilon_\infty = \frac{\Delta\varepsilon}{\{1 + (i\omega\tau_{\text{HN}})^\alpha\}^\beta} \quad (1)$$

where, ω is the frequency in radians/sec, α and β are parameters corresponding to the width and asymmetry of the relaxation time distributions, respectively, τ_{HN} is the HN relaxation time, and $\Delta\varepsilon = \varepsilon_S - \varepsilon_\infty$ the dielectric strength (with ε_S and ε_∞ being the real part of the permittivity when $\omega \rightarrow 0$ and $\omega \rightarrow \infty$, respectively). The relaxation time and frequency ($f_{\text{max}} = 1/\tau_{\text{max}}$) of the HN individual ε^* curves were calculated according to eq. (2)¹⁹:

$$\tau_{\text{max}} = \tau_{\text{HN}} \left[\frac{\sin\left(\frac{\pi(\alpha_{\text{NH}})\beta_{\text{NH}}}{2(\beta_{\text{NH}} + 1)}\right)}{\sin\left(\frac{\pi(\alpha_{\text{NH}})}{2(\beta_{\text{NH}} + 1)}\right)} \right]^{1/\alpha_{\text{NH}}} \quad (2)$$

The ε'' curves were also fitted to Foyss–Kirkwood [eq. (3)] functions in the temperature domain²²:

$$\varepsilon'' = \frac{\varepsilon''_{\text{max}}}{\cosh\left\{\text{bea} \left(\frac{1}{T} - \frac{1}{T_{\text{max}}}\right)\right\}} \quad (3)$$

where, $\text{bea} = mE_a/R$ is a parameter dependent on the activation energy of the relaxation (E_a), $\varepsilon''_{\text{max}}$ is the maximum in the ε'' curve, and T_{max} is the maximum relaxation temperature at a given frequency (f).

At sufficiently high temperatures, ohmic conduction due to charge carriers (σ^*) frequently dominates the loss contribution at low frequencies, potentially masking dielectric relaxations. In order to discriminate dielectric and conductivity effects, the conduction-free dielectric loss, $\varepsilon''_{\text{NC}}$, was also determined by eq. (4)²³:

$$\varepsilon''_{\text{NC}} = \varepsilon'' - \frac{\sigma_0}{\varepsilon_0 2\pi f S} \quad (4)$$

where, f is the frequency in Hertz, σ_0 is a pre-exponential coefficient, and S is an exponent normally close to 1.

The thermal activation of the dielectric phenomena was analyzed in Arrhenius maps using the maxima temperature of the relaxations at each frequency or temperature, being described by either linear [eq. (5)]

$$f_{\text{max}} = f_0 \exp\left(\frac{-E_a}{R \cdot T}\right) \quad (5)$$

where, E_a is the apparent activation energy and f_0 is a pre-exponential term.

RESULTS AND DISCUSSION

Thermal Results

The area below the thermograms from 50°C to 160°C, normalized by 291 J/g as the enthalpy of melting of a 100% crystalline UHMWPE, gave the crystallinity percentages for each material. Both the crystallinity and the peak melting point of 0.1 wt % vitamin E-blended polymer increased with radiation dose (Table I). This trend was similar to previous reports for this resin without vitamin E.^{24,25}

On the other hand, the incorporation of vitamin E at high concentrations by diffusion (range 1.5–7.9 wt %) provoked a drop in the crystallinity content and lamellar thickness (Table I). This last effect may be a consequence of the rise in transition temperature (T_m), which according to the Thomson–Gibbs equation involves in increase in lamellar thickness, L_c :

$$T_m = T_{m0} (1 - 2\sigma/L_c \rho_c \Delta H_{m0})$$

where, T_m is the melting point of the polymer; T_{m0} is the equilibrium melting point of a perfect crystalline polyethylene; σ is the specific surface energy; ρ_c is the crystallinity phase density, and ΔH_{m0} is the enthalpy of melting of a perfect crystalline polyethylene.

Table III. Influence of Vitamin E Content on AC Conductivity Parameters Obtained by eq. (4) in GUR1050-Y wt %

| T (°C) | log(σ_0) (S cm ⁻¹) | | | | S | | | |
|--------|---|----------|----------|----------|--------|----------|----------|----------|
| | 0 wt % | 1.5 wt % | 4.4 wt % | 7.9 wt % | 0 wt % | 1.5 wt % | 4.4 wt % | 7.9 wt % |
| 130 | -14.08 | -13.60 | -13.82 | -12.72 | 1.0 | 1.00 | 0.96 | 0.90 |
| 123 | -14.27 | -14.13 | -14.97 | -13.27 | 1.0 | 1.00 | 0.69 | 0.84 |
| 117 | -14.72 | | -15.72 | -13.61 | 1.0 | | 0.76 | 0.81 |
| 111 | -14.42 | | -15.12 | -13.76 | 1.0 | | 1.00 | 0.81 |
| 105 | | | -15.05 | -14.06 | | | 1.00 | 0.70 |
| 99 | | | | -14.03 | | | 1.00 | 0.79 |
| 93 | | | | -13.93 | | | | 0.98 |
| 87 | | | | -14.02 | | | | 0.94 |
| 81 | | | | -14.16 | | | | 0.84 |
| 75 | | | | -14.09 | | | | 1.00 |
| 69 | | | | -14.25 | | | | 0.93 |
| 63 | | | | -14.19 | | | | 1.00 |
| 57 | | | | -14.52 | | | | 0.87 |
| 51 | | | | -14.57 | | | | 1.00 |

Finally, the reduction in crystallinity content due to vitamin E has been also reported by Oral et al.,²⁶ this effect being intensified when the temperature of the diffusion process approaches the melting temperature.

Dielectric Results

The Dielectric Behavior of Resins Without Irradiation. Figure 1(a) shows the ϵ'' response corresponding to the GUR1050 sample, as a function of the temperature and at different

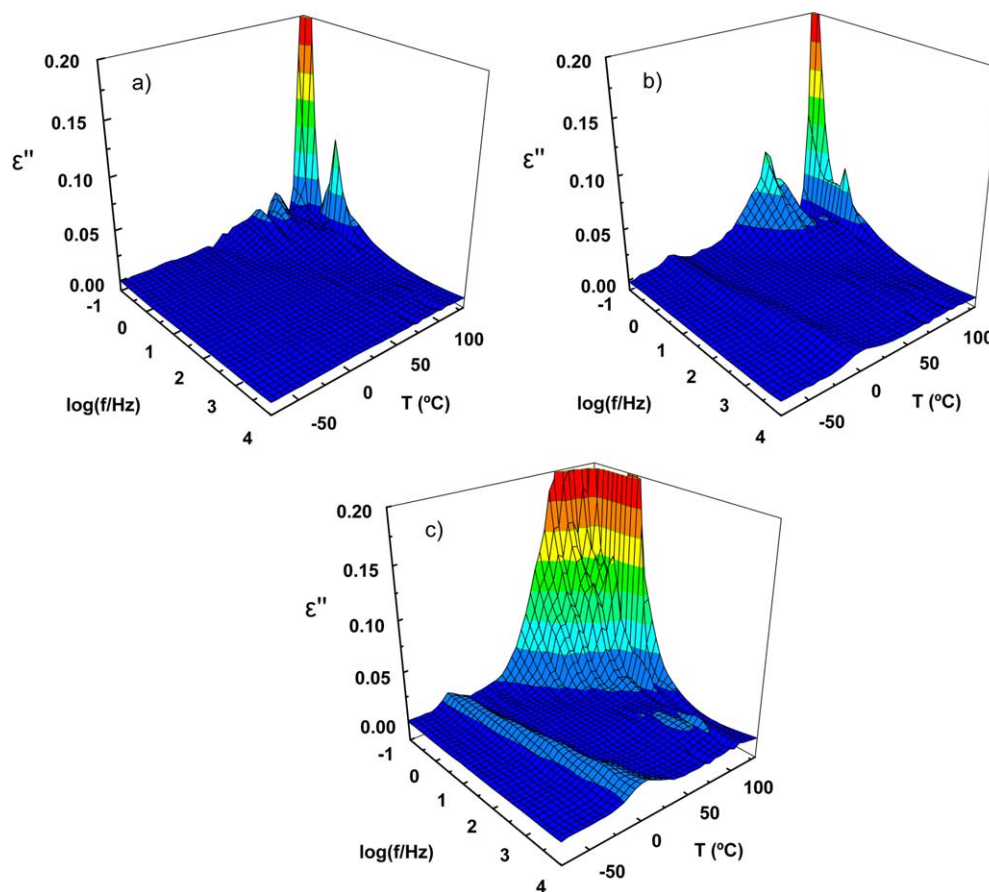


Figure 2. 3D plots showing the frequency/temperature dependence of the ϵ'' response of (a) GUR1050-VE1.3, (b) GUR1050-VE4.4, and (c) GUR1050-VE7.9. [Color figure can be viewed in the online issue, which is available at wileyonlinelibrary.com.]

frequencies. At the lowest temperatures, the ϵ'' values are negligible, and only at temperatures above 0°C and at frequencies lower than 10 Hz, some relaxations appeared. At the highest temperatures and lowest frequencies, the ϵ'' values rise, exceeding the range typical of dielectric relaxation and suggesting the existence of AC conductivity in that region. In case of GUR1050VE0.1 specimen, the isochrone $\epsilon''(T)$ curves show [Figure 1(b)] several dielectric processes overlapped also with an AC conductivity term. The presence of this small amount of vitamin E embossed the dielectric behavior in ϵ'' and additionally the appearance of a slight shift of the temperature of the ϵ'' maximum to lower temperatures. The subtraction of conductivity term in both resins was performed by applying eq. (4) in the frequency domain. The values of σ_0 and S at different temperatures are summarized in the first and fifth column of Table II, respectively for GUR1050VE0.1, while data for GUR1050 are presented in Table III. Although after subtraction the values of $\epsilon''(T, \omega)$ do not allow obtaining a reliable quantitative analysis of the relaxations present, dielectric measurements allow to detect some relaxations.

The γ relaxation is not observed in any of the materials, because it appears in the polyethylenes at around -83°C , which is below the lowermost temperature used during our experiment. The α and α' relaxation, generally attributed to the relaxation mechanisms in the crystalline region, are observed in the unirradiated or uncrosslinked resins, GUR1050 and GUR1050-VE0.1. The common β relaxation that appears in some polyethylenes at around -25°C is not detected in the neat GUR1050. This relaxation is widely accepted to be related to the relaxation of chain units in the interfacial zone between the lamella and its surrounding amorphous region.²⁷ Mechanisms associated to chain-end, fold-surface, branch-point molecular motions, and chain rotation are involved in this relaxation.⁵ Therefore, higher crystalline content and the prevalent structural linearity of Nitta and Tanaka²⁸ may result in the absence of this relaxation. However, in a recent work by Puértolas et al.,²⁹ this

β relaxation was weakly detected in GUR1050 by means of dynamic mechanical thermal analysis.

Influence of the Irradiation Dose. The dielectric behavior of the irradiated materials was similar to that observed in the unirradiated material with respect to temperature and frequency. There were also two recognizable peaks at low frequencies, whose peaks do not follow a temperature/frequency dependence expected for relaxations. Additionally, a conductivity term is also present, which was also assessed by means of the same procedure described for the unirradiated material. The corresponding σ_0 and S values as a function of the temperature are included in Table II. The results indicated an increase in the conductivity values, σ_0 , at the highest irradiation doses, reaching a value close to $\log \sigma_0 = -12$, whereas all the values of the S parameter were close to 1. These AC conductivity outcomes showed higher radiation dose dependence than those found by Mathad et al.³⁰

This conductivity could be associated with an increase in the carrier charge density as a result of an increase in free radicals, unsaturated bonds, and defects, which may be generated by irradiation. However, the different mobility of the carrier in the amorphous and crystalline regions could be taken as a synergistic effect on the different AC conductivity in the irradiated polyethylenes.

Influence of the Vitamin E Concentration. Figure 2 is a 3D plot, which illustrates the ϵ'' dependence of GUR1050-VEY% series with $Y = 1.3, 4.4,$ and 7.9 wt % of vitamin E content in the temperature and frequency range of interest. The plots show the presence of a relaxation at the lowest temperatures from -50°C to 20°C , which is clearly visible for the specimens with $Y = 4.4$ and 7.9 wt %, but cannot be detected in the GUR1050-VE1.3 samples, suggesting that the relaxation must be related to the presence and amounts of vitamin E. From Figure 2(a–c) can also be observed other process at higher temperatures and frequencies, which will be denoted as α relaxation, rather a prominent conductivity is also present, especially above 20°C , which overlapped with the α relaxation.

The analysis of this process at the lowest frequencies applying eq. (4) allows us to determine the σ_0 and S parameter of the conductivity term, which are summarized in Table III. At the same temperature, the conductivity is considerably higher in the sample with the highest vitamin E contents, $Y = 7.9$ wt %, but the values are still lower those of the samples submitted to high dose irradiation.

In general, the AC conductivity presented a less significant contribution when vitamin E was incorporated into polyethylene by diffusion, than when the polyethylene resins underwent electron beam irradiation. In order to study the influence of the microstructure aspects on the AC conductivity, the first conclusion we deduce is that this AC conductivity is independent of the crystallinity, because the effects of electron beam irradiation and vitamin E content go in opposite trends respect to the influence on crystallinity. In Figure 3, we plot the $\log \sigma$ at different temperatures and corresponding to materials of both series (X and Y) versus their transition temperatures. According to this figure and taking

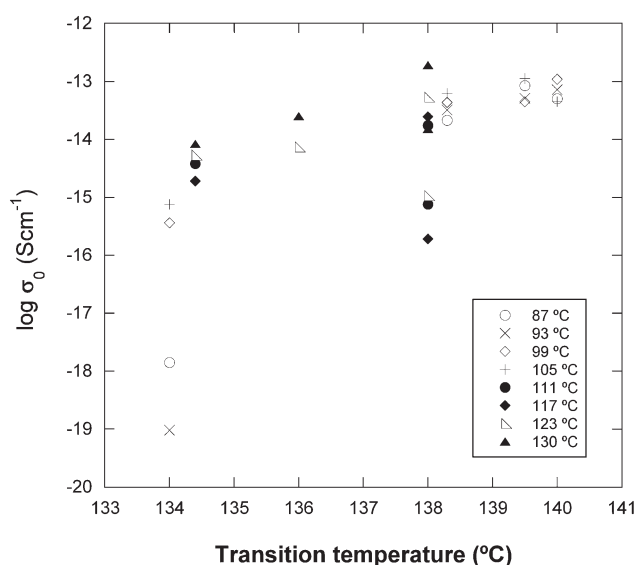


Figure 3. AC conductivity of materials (X and Y series) at different temperatures above 87°C versus transition temperatures of these materials.

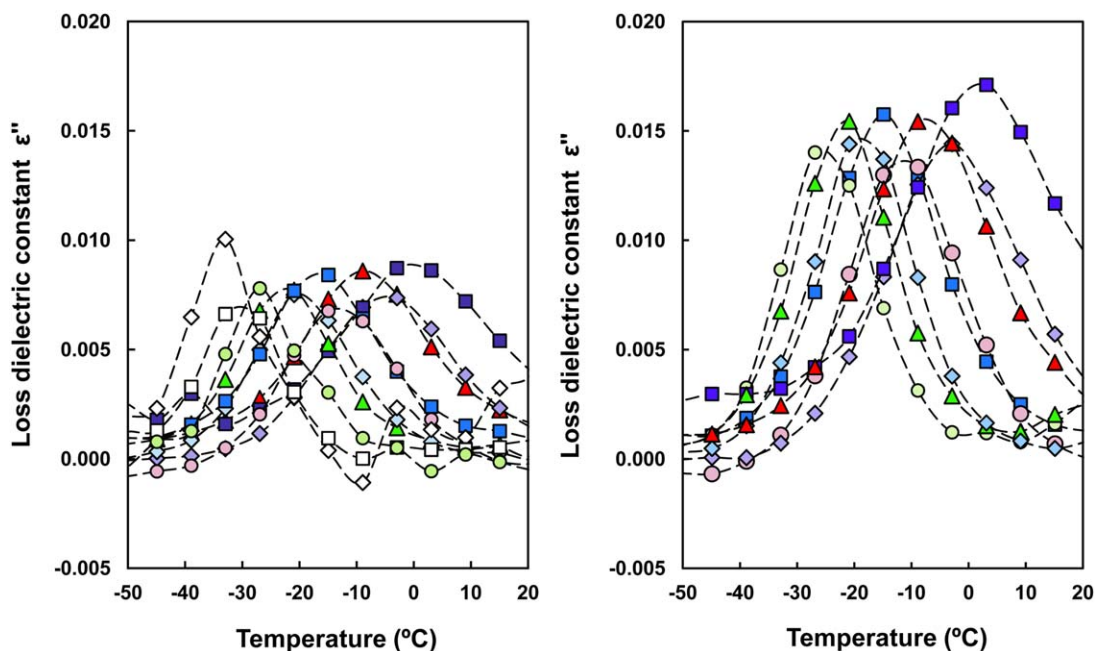


Figure 4. Temperature dependence of the ϵ'' response of GUR1050-VE4.4 (a) and GUR1050-VE7.9 (b) in the low temperature range, at different frequencies (in Hz): \blacksquare : 1×10^4 , \blacklozenge : 3×10^3 , \blacktriangle : 1×10^3 , \bullet : 3×10^2 , \blacksquare : 1×10^2 , \blacklozenge : 3×10^1 , \blacktriangle : 1×10^1 , \bullet : 3×10^0 , \square : 3×10^{-1} , and \diamond : 1×10^{-1} . [Color figure can be viewed in the online issue, which is available at wileyonlinelibrary.com.]

Table IV. Parameters Obtained after Fitting the ϵ'' Curves to Havriliak–Negami Expressions

| T (°C) | GUR1050-VE4.4 | | | | GUR1050-VE7.9 | | | |
|----------|--------------------------------------|---------------------------------------|----------|---------|--------------------------------------|---------------------------------------|----------|---------|
| | τ_{\max} (sec·10 ²) | $\Delta\epsilon''$ (10 ²) | α | β | τ_{\max} (sec·10 ²) | $\Delta\epsilon''$ (10 ²) | α | β |
| -32 | 314,000 | 7.27 | 0.76 | 0.34 | | | | |
| -26 | 11,300 | 54.9 | 0.82 | 0.29 | 14,900 | 0.360 | 0.51 | 0.54 |
| -20 | 591 | 2.81 | 0.45 | 0.69 | 1,280 | 1.02 | 0.44 | 0.78 |
| -14 | 123 | 0.903 | 0.59 | 0.37 | 185 | 0.765 | 0.62 | 0.30 |
| -8 | 16.4 | 0.0897 | 0.49 | 0.46 | 19.3 | 0.306 | 0.71 | 0.11 |
| -2 | 1.06 | 0.00579 | 0.44 | 0.60 | | | | |

into account the relation of T_m and lamellar thickness (see Thomson–Gibbs equation), it seems that the lamellar thickness is a relevant microstructural factor for the AC conductivity, in line with the conclusion given by Mandelkern et al.²⁷

The subtraction of the conductivity term from the isothermal curves, $\epsilon''(f)$ above 51°C, revealed the presence of the α process, which is especially visible in the case of GUR1050-VE7.9, and whose intensity increases with increasing temperature.

Table V. Parameters Obtained After Fitting the ϵ'' Curves to Fouss–Kirkwood Expressions

| f (Hz) | GUR1050-VE4.4 | | | GUR1050-VE7.9 | | |
|----------|--------------------------------------|-----------|-----------------|--------------------------------------|----------|-----------------|
| | ϵ_{\max} (10 ³) | bea | T_{\max} (°C) | ϵ_{\max} (10 ³) | bea | T_{\max} (°C) |
| 3 | 7.77 | 10,260.14 | -26.4 | 14.53 | 8,607.12 | -30.4 |
| 10 | 7.87 | 8,118.90 | -22.6 | 14.72 | 8,910.59 | -25.0 |
| 30 | 7.66 | 8,656.39 | -19.5 | 15.59 | 8,253.45 | -22.0 |
| 100 | 8.37 | 6,668.58 | -16.4 | 15.30 | 8,653.12 | -18.8 |
| 300 | 7.35 | 9,313.94 | -12.8 | 15.81 | 7,379.79 | -15.4 |
| 1,000 | 8.39 | 6,184.72 | -8.9 | 14.52 | 8,699.07 | -11.8 |
| | | | | 15.43 | 6,383.33 | -7.7 |

Table VI. Activation Energies, E_a , Calculated for the Low Temperature Relaxation in GUR1050 – Y wt %

| Method | GUR1050-VE4.4 | | | GUR1050-VE7.9 | | |
|------------------|------------------------|---|--------|------------------------|---|--------|
| | Temperature range (°C) | Activation energy (kJ mol ⁻¹) | R^2 | Temperature range (°C) | Activation energy (kJ mol ⁻¹) | R^2 |
| Havriliak–Negami | –26/–8 | 192.46 | 0.9867 | –32/–2 | 202.51 | 0.9987 |
| Fouss–Kirkwood | –26/–8 | 182.32 | 0.9988 | –32/–2 | 184.65 | 0.9962 |

The results also point out that the isothermal curves undergo changes in the peak shape in a more significant way than the peak position, with an additional growing component at around $f = 3$ Hz. However, the uncertainty of the experimental values of ϵ'' does not allow a reliable information of this complex process.

Dielectric response at lower temperatures was not affected by conductivity; therefore the analysis of this relaxation was less complicated. Henceforth, this relaxation will be denoted as β relaxation. Figure 4 shows the isochronal curves. Isothermal curves values were fitted to HN [eqs. (1) and (2)] and isochronal ones by Fouss–Kirkwood [eq. (3)] equations, respectively, and the parameters obtained are indicated in Tables IV and V. The relaxation times (τ_{\max}) and temperatures (T_{\max}) determined with eqs. (1), (2), and (3), respectively, were used to plot the corresponding Arrhenius maps in Figure 5. The β relaxations show linear dependence with the temperature, indicating low influence of cooperative motions in the dielectric response, being in good coherence with the results obtained by NH and FK because the error band was lower than 10%. Activation energies calculated following eq. (6) are summarized in Table IV.

Few works have focused on the dielectric contribution of α -tocopherol, which is the compound incorporated into UHMWPE by blending into resin powder before consolidation or diffusion into consolidated solid forms. This tocopherol is a glass-forming material, with a glass transition temperature close to -33°C . The introduction of 0.1 wt % vitamin E by blending in the polyethylene does not modify the previous behavior regarding the absence of the β relaxations. However, in the nonirradiated vitamin E-diffused polyethylene, above 1.5 wt % of vitamin E these materials exhibit β relaxation, which was strengthened by increasing the amount of vitamin E doping and was shifted toward low temperatures. These results corroborate with earlier results on the effect of diffused vitamin E on the relaxation behavior of UHMWPE obtained by dynamic mechanical thermal analysis.²² On the other hand, the activation energy, which is around 184 kJ mol^{-1} by means of the Fouss–Kirkwood approach, is close to the previously determined from T_{\max} of the isochrone curves, 188 kJ mol^{-1} at 9 wt % in that work. Regardless of the used technique, dielectric relaxation spectroscopy or dynamic mechanical thermal analysis, the rising activation energy registered for increasingly higher antioxidant concentrations seem to discard any plasticization effect of vitamin E in spite of the temperature shift of the β relaxation.

It is difficult to associate the origin of this β relaxation with the presence of vitamin E. A possible mechanism could be related to the microstructural changes induced by the annealing at 120°C , which is used during the incorporation of vitamin E

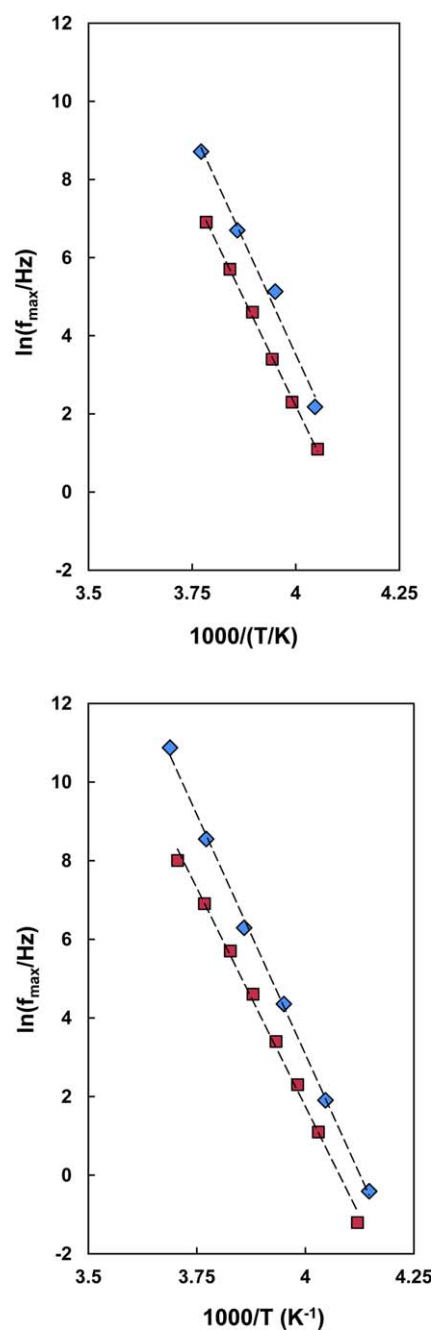


Figure 5. Arrhenius maps corresponding to the GUR1050-VE4.4 (a) and GUR1050-VE7.9 (b) samples obtained from the application of the Fouss–Kirkwood (■) and Havriliak–Negami (◆) equations. [Color figure can be viewed in the online issue, which is available at wileyonlinelibrary.com.]

into polyethylene.^{31,32} Although chain scissions take place initially in the amorphous zone, the morphological changes are mainly produced in the crystalline–amorphous interface. Thus, these changes together with possible recrystallization of newly formed chains may modify crystalline–amorphous interface in the presence of high concentration of vitamin E and contribute to the induction of a β relaxation.

CONCLUSIONS

The α and α' relaxation are overlapped by AC conductivity that is present at about 60°C for all the studied materials. This AC conductivity increased clearly when the polyethylene resins underwent electron beam irradiation and less significantly when vitamin E was incorporated into polyethylene by diffusion from its respective basic resins. The effects of electron beam irradiation and vitamin E content go in opposite trends. The lamellar thickness is a relevant microstructural factor of α and α' relaxation.

The β relaxation is not detected in the neat GUR1050 and 0.1 wt % vitamin E by blending in the polyethylene. However, in the nonirradiated vitamin E-diffused polyethylene, above 1.5 wt % of vitamin E, these materials exhibit β relaxation, which was strengthened by increasing the amount of vitamin E doping and was shifted toward low temperatures. A possible mechanism could be related to the microstructural changes induced by the incorporation of vitamin E-infused polyethylene, simultaneously to the annealing process at 120°C.

ACKNOWLEDGMENTS

Research funded by the Comisión Interministerial de Ciencia y Tecnología (CICYT), Spain. Project MAT 2010–16175 from the Ministerio de Ciencia e Innovación. The authors also acknowledge support from Project ENE2011–28735–C02–01 and Mr. Teruel Grant GRISOLIAP/2012/056.

REFERENCES

1. Boyd, R. H.; Smith, G. D. *Polymer Dynamics and Relaxation*; Cambridge University Press: Cambridge, 2007.
2. Schmieder, K.; Wolf, K.; *Kolloid Z* **1953**, *134*, 149.
3. Oakes, W. G.; Robinson, D. W. *J. Polym. Sci.* **1954**, *14*, 505.
4. Flocke, H. A. *Kolloid Z* **1962**, *180*, 118.
5. Suljovrujic, E. *Radiat. Phys. Chem.* **2010**, *79*, 751.
6. Gilchrist, J.; Le, G. *Cryogenics* **1979**, *19*, 281.
7. Yang, S.; Benitez, R.; Fuentes, A.; Lozano, K. *Compos. Sci. Technol.* **2007**, *67*, 1159.
8. Suljovrujic, E.; Kac̄arevic-Popovic, Z.; Kostoskia, D.; Dojcōeilovic, J. *Polym. Degrad. Stab.* **2001**, *71*, 367.
9. Kurtz, S. M. *The UHMWPE Biomaterials Handbook: Ultra-High Molecular Weight Polyethylene in Total Joint Replacement and Medical Devices*, 2nd ed.; Academic Press: Burlington, MA, 2009.
10. Cumming, C. S.; Lucas, E. M.; Marro, J. A.; Kieu, T. M.; DesJardins, J. D. *Adv. Space Res.* **2011**, *48*, 1572.
11. Zhong, W. H.; Millert, J. *International Conference on Smart Materials and Nanotechnology in Engineering*; V6423:Z4231, Trans Tech Publications Ltd, Switzerland, 2011.
12. Cao, X. Z.; Xue, X. X.; Jiang, T.; Li, Z. F.; Ding, Y. F.; Li, Y.; Yang, H. *J. Rare Earths* **2010**, *28S1*, 482.
13. Kaloshkin, S. D.; Tcheerdyntsev, V. V.; Gorshenkov, M. V.; Gulbin, V. N.; Kuznetsov, S. A. *J. Alloy. Compd.* **2012**, *536S*: S522.
14. Muratoglu, O. K.; Bragdon, C. R.; O'Connor, D.; Perinchief, R. S.; Estok, D. M.; Jasty, M.; Harris, W. H. *J. Arthroplast.* **2001**, *16*, 24.
15. Goldman, M.; Gronsky, R.; Pruitt, L. *J. Mat. Sci. Mat. Med.* **1998**, *98*, 207.
16. Gómez-Barrena, E.; Puértolas, J. A.; Munuera, L.; Konttinen, Y. *Acta Orthop.* **2008**, *79*, 832.
17. Bracco, P.; Oral, E. *Clin. Orthop. Relat. Res.* **2011**, *469*, 2286.
18. ASTM F2625. *Standard Test Method for Measurement of Enthalpy of Fusion, Percent Crystallinity, and Melting Point of Ultra-High-Molecular Weight Polyethylene by Means of Differential Scanning Calorimetry*; ASTM: West Conshohocken, PA, 2010.
19. Havriliak, S.; Negami, S. A. *Polymer* **1967**, *8*, 161.
20. Havriliak, S.; Negami, S. *Dielectric and Mechanical Relaxation in Materials*; Hanser: Munich, 1997.
21. Ngai, K. L.; Schonhals, A.; Schlosser, E. *Macromolecules* **1992**, *25*, 4915.
22. Fuoss, R. M.; Kirkwood, J. G. *J. Am. Chem. Soc.* **1941**, *2*, 385.
23. Brotthcher, C. J. F.; Borderwijk, P. *Theory of Electric Polarization*, 2nd ed.; Elsevier: Amsterdam, 1978.
24. Premnath, V.; Harris, W. H.; Jasty, M.; Merrill, E. W. *Biomaterials* **1996**, *17*, 1741.
25. Medel, F. J.; García-Álvarez, F.; Gómez-Barrena, E.; Puértolas, J. A. *Polym. Degrad. Stab.* **2005**, *88*, 435.
26. Oral, E.; Wannomae, K. K.; Rowell, S. L.; Muratoglu, O. K. *Biomaterials* **2007**, *28*, 5225.
27. Mandelkern, L.; Glotin, M.; Popli, R. *J. Polym. Sci. Polym. Phys.* **1981**, *19*, 435.
28. Nitta, K. H.; Tanaka, A. *Polymer* **2001**, *42*, 1219.
29. Puértolas, J. A.; Martínez-Morlanes, M. J.; Mariscal, M. D.; Medel, F. J. *J. Appl. Polym. Sci.* **2011**, *120*, 2282.
30. Mathad, R. D.; Kumar, H. G. H.; Sannakki, B.; Sanjeev, G.; Sarma, K. S. S.; Francis, S. *Radiat. Effect. Defect. Solid.* **2010**, *165*, 277.
31. Ribes-Greus, A.; Díaz-Calleja, R. *J. Appl. Polym. Sci.* **1989**, *38*, 1127.
32. Ribes-Greus, A.; Díaz-Calleja, R. *J. Appl. Polym. Sci.* **1989**, *37*, 2549.